

RSC Advances



This is an *Accepted Manuscript*, which has been through the Royal Society of Chemistry peer review process and has been accepted for publication.

Accepted Manuscripts are published online shortly after acceptance, before technical editing, formatting and proof reading. Using this free service, authors can make their results available to the community, in citable form, before we publish the edited article. This *Accepted Manuscript* will be replaced by the edited, formatted and paginated article as soon as this is available.

You can find more information about *Accepted Manuscripts* in the [Information for Authors](#).

Please note that technical editing may introduce minor changes to the text and/or graphics, which may alter content. The journal's standard [Terms & Conditions](#) and the [Ethical guidelines](#) still apply. In no event shall the Royal Society of Chemistry be held responsible for any errors or omissions in this *Accepted Manuscript* or any consequences arising from the use of any information it contains.

Introduction of a α,β -unsaturated carbonyl conjugated pyrene-lactose hybrid as a fluorescent molecular probe for micro-scale anisotropic media

Ivy Sarkar^a, Arasappan Hemamalini^b, Thangamuthu Mohan Das^{*b,c}, Ashok Kumar Mishra^{*a}

^a Department of Chemistry, Indian Institute of Technology Madras, Chennai – 600 036, India

^b Department of Organic Chemistry, University of Madras, Guindy Campus, Chennai - 600 025,
India

^c Department of Chemistry, School of Basic and Applied Sciences, Central University of Tamil
Nadu, Thiruvarur – 610 101, India

Abstract:

A new fluorescent lactose molecule (pyd-lact) (*E*)-1-(galactose- β -(1 \rightarrow 4)- β -D-glucopyranosyl)-4-(1-pyrene)-but-3-en-2-one, has been synthesized by attaching 1-pyrene-but-3-ene-2-one with lactose. Extended π -conjugation removes the emission forbidden-ness of pyrene which results in the broad spectrum. Detailed photo-physical studies in homogeneous media show the sensitivity of ICT (intra molecular charge transfer) emission towards medium polarity. Unlike pyrene, pyd-lact is more soluble in water at probe's concentration (10 μ M), because of the attached disaccharide. Thus, the usage of pyd-lact as an aqueous probe is found to be advantageous over pyrene. Using the polarity sensitivity of fluorescence parameters (intensity, shift of emission maximum, anisotropy, lifetime) micro-heterogeneity of anisotropic media such as β -CD, bile salts, pluronic P123 have been monitored. In contrast to pyrene-3-carboxaldehyde which is often used as a hydrophobic fluorescent molecular probe, pyd-lact reports from the interfacial regions of micro-heterogeneous media.

Key words:

1-pyrene-but-3-ene-2-one, lactose, solubility, fluorescence, micro-heterogeneity.

Introduction:

Fluorescence is an important spectroscopic tool in the field of bio and bio-mimic systems. For biological applications fairly water soluble fluorophores are needed as water is the unique solvent in bio-systems. But, a major problem of several organic molecular probes is insolubility in water which limits their bio-applicability. Highly hydrophobic pyrene and its non-polar derivatives often suffer from this insolubility problem (e.g. pyrene is soluble in water at 0.64 μM).¹ As for example, pyrene-3-carboxaldehyde, a sparingly soluble fluorophore, is one of the most useful derivative of pyrene due to its polarity sensitivity.²⁻⁹ Solubility of this kind of probes in water can be improved by functionalization or conjugation with polar groups or molecules, respectively. Functionalization of pyrene with polar $-\text{SO}_3^-$ and $-\text{OH}$ groups increase aqueous solubility of pyranine.⁹ Likewise, sugar molecules are highly suitable for conjugation due to their bio-compatibility.¹⁰ It has been found that, applicability of conventional fluorescent molecular probes can be increased by suitable conjugation with different molecules of interest. Conjugation of this kind helps to localize the probe at specific site of interest in different micro-heterogeneous media.^{11,12} These probes are often referred as ‘system probes’ which are known for providing more information and less perturbation than the standard probes.^{11,12} For last couple of decades, several system probes attached with steroids, lipids, sugar molecules, proteins, DNA fragments have been introduced to investigate the relevant bio-functionalities.¹⁰⁻²³ Along with good probing ability these conjugations can also increase compatibility of the probe molecules with the corresponding organized systems. As for example, use of fluorescent carbohydrates help to

increase the sensitivity of capillary electrophoresis (CE) of oligosaccharides.^{21,22} Likewise, fluorescent cyclodextrin derivatives are known for their good sensing ability.^{16,23} Extending the versatility of fluorescent carbohydrates, in our recent work,²⁴ we have introduced a conjugate involving pyrene and a protected glucose unit, 1-(4,6-*O*-butylidene- β -*D*-glucopyranosyl)-4-(1-pyrene)-butan-2-one (pyd-glc) for micro-heterogeneous media. Protection of the glucose moiety in this molecule allowed polarity modulation so as to impart better partitioning of the molecule to non-polar micro-heterogeneous media.²⁴

The present work introduces a pyrene derivative conjugated to a highly hydrophilic lactose unit, (*E*)-1-(galactose- β -(1 \rightarrow 4)- β -*D*-glucopyranosyl)-4-(1-pyrene)-but-3-en-2-one (pyd-lact) (Figure 1). As the structure shows, the basis fluorophoric unit in pyd-lact is an extended π -conjugated system with an electron deficient carbonyl group in one end which would have photo-physical properties significantly different from that of pyrene (Figure 1). In addition, the enhanced hydrophilicity contrast within the molecule could enable efficient localization of pyd-lact at hydrophobic-hydrophilic interfaces of the micro-heterogeneous media, unlike pyrene-3-carboxaldehyde which is a hydrophobic probe.⁶ Pyrene carbonyl compounds (pyrene-3-carboxaldehyde, 1-acetylpyrene, 1-pyrenecarboxylic acid, 1-methoxycarbonylpyrene) are well known for their unique photo-physical properties and have widely been used in various fields.² As for example, pyrene-3-carboxaldehyde is a popular probe for micelles,²⁻⁸ 1-acetylpyrene has been used as light-harvesting antennas,^{2,25,26} 1-pyrenecarboxylic acid is a pH probe^{2,27,28,29} and 1-methoxycarbonylpyrene has been used as a signal sensitizer.^{2,30} Pyrene-3-carboxaldehyde and 1-acetylpyrene are known for their low fluorescence ($k_{nr} = k_{ISC} \gg k_r$), whereas, 1-pyrenecarboxylic acid and 1-methoxycarbonylpyrene are known for high fluorescence ($k_r \gg k_{nr}$).² The interesting

photo-physics of pyrene carbonyl compounds along with their versatile applications have made this molecule worthy for investigation.

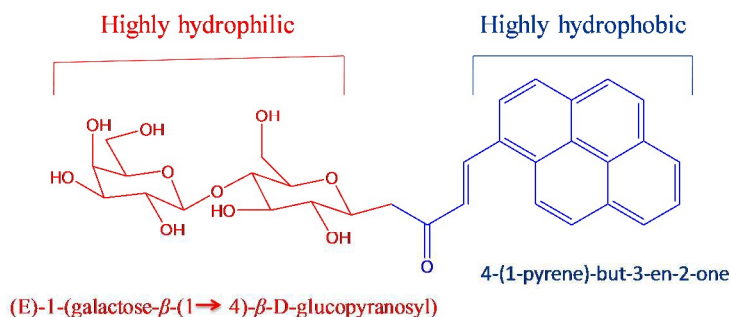


Figure 1: Molecular structure of (*E*)-1-(galactose-β-(1→4)-β-D-glucopyranosyl)-4-(1-pyrene)-but-3-en-2-one, (pyd-lact).

Cyclic oligosaccharide, β-cyclodextrin (β-CD) composed of D(+)-glucopyranose units has been used as a sugar based anisotropic media to monitor the sensitivity of pyd-lact.³¹⁻³⁵ These toroidal cyclodextrins show micro-heterogeneity because of their hydrophilic outer surface containing –OH groups and hydrophobic inner core.³¹ Due to the inclusion complex forming ability, cyclodextrins (α, β, γ - CDs) are being used in drug delivery systems, food industries, environmental protection, toxicity reduction of medicines etc.^{32,34} Bile salts and pluronic micro-heterogeneous media have been used as non-sugar bio-anisotropic media to analyze the potential of pyd-lact. Bile salts are naturally occurring surfactants which help to digest fat in animal hepatobiliary system.³⁶ Hydrophobic steroidal backbone in one face and hydrophilic –COOH and –OH groups in opposite face imparts facial polarity. Drug-bile conjugates have been used in several occasions to improve the intestinal absorption of poorly absorbed drugs.^{37,38} Pluronic P123 (PEO₂₀-PPO₇₀-PEO₂₀) is a tri-block co-polymer composed of hydrophilic poly (ethylene oxide) (PEO) and hydrophobic poly (propylene oxide) (PPO) units.^{39,40,41} Anhydrous hydrophobic core region of PPO units helps in solubilizing water insoluble drug molecules.³⁹ On

the other hand, hydrophilic corona region of PEO units keeps the micelle dispersed in water and ensures drug availability to the target cells.³⁹ Now a days, 'polymer therapeutics' has been successfully used in drug and gene delivery, diagnostic imaging, cancer treatment etc.⁴⁰

The particular aims of this work are, (i) to synthesis and characterize a newly modified pyrene derivative (*E*)-1-(galactose- β -(1 \rightarrow 4)- β -D-glucopyranosyl)-4-(1-pyrene)-but-3-en-2-one, (pyd-lact) with considerable solubility, (ii) to study its photo-physics in homogeneous media and (iii) to study its response in sugar-based micro-heterogeneous media, β -CD and also in other non-sugar based media like bile salts (NaC, NaDC) and pluronic (P123).

Material and Methods:

Materials: β -CD, pluronic P123 was purchased from Sigma Chemical Co. (Bangalore, India). Sodium di-hydrogen phosphate, di-sodium hydrogen phosphate were purchased from Merck Specialties Pvt. Ltd. (Mumbai). Bile salts, sodium cholate (NaC) and sodium deoxy cholate (NaDC) were purchased from S. D. Fine Chemical Company, India. Triple distilled water used for all experiments was prepared by using KMnO_4 and NaOH. All other solvents used were of spectroscopic grade.

0 to 16 mM solutions of β -CD in pH \sim 7.4 phosphate buffer were used for this study. Fresh stock solutions were prepared for all the experiments. NaC and NaDC concentrations were varied from 0-48 and 0-18 mM, respectively. pH of the solutions were kept at \sim 7.4 with 50 mM phosphate buffer, similar to the physiological condition. Fresh bile salt solutions were used to avoid aging. 10% (w/v) solution of pluronic P123 in triple distilled water was used for this experiment. Polymeric solution was kept in fridge to ensure complete dissolution. Then probe

solution was added with the prepared polymeric solution and kept over-night to ensure homogeneity.

1 mM methanolic solution of pyd-lact was used as stock solution for all experiments. After evaporating methanol triple distilled water was added and sonicated to get a stock solution of 50 μM probe in water. Final probe concentration was maintained at 10 μM .

Photophysical studies: Fluorescence measurements were done by using Fluoromax 4 (Horiba Jobin Yvon) spectrofluorimeter having 150 W Xenon lamp as excitation source. Steady state fluorescence anisotropy (r_{ss}) was determined by using the following equation.⁴²

$$r_{ss} = \frac{I_{VV} - GI_{VH}}{I_{VV} + 2GI_{VH}}, \quad G = \frac{I_{HV}}{I_{HH}}$$

where, I_{VV} and I_{VH} are fluorescence intensities and subscripts V (vertical) and H (horizontal) signify orientation of excitation and emission polarizer and G is the instrument correction factor.

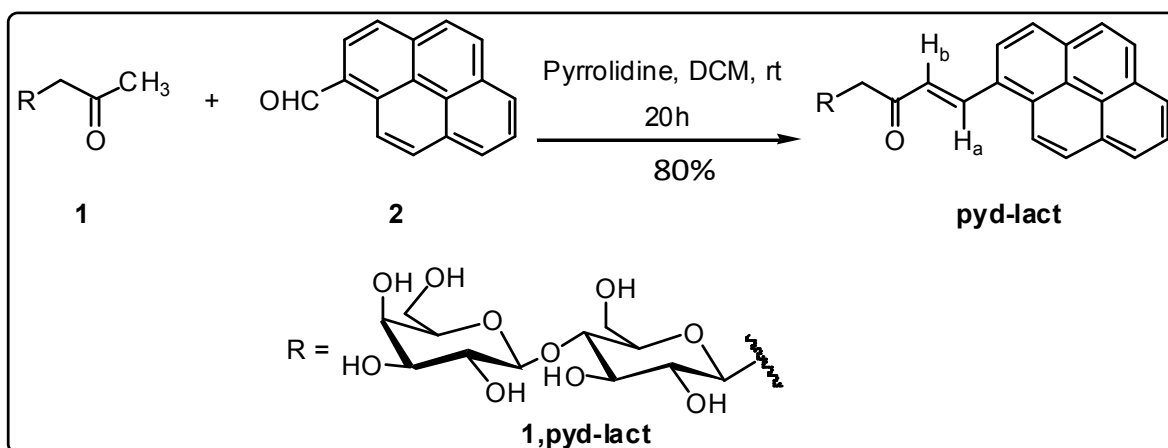
Data acquisition was done by Horiba Jobin Yvon TCSPC lifetime instrument in time-correlated single-photon counting arrangement. Nano-LED of 370 nm was used as excitation source. The pulse repetition rate was set to 1 MHz. Instrumental full width at half-maxima of the 370 nm LED, including the detector response was measured to be ~ 1.1 ns. The instrument response function was collected by using scattered medium, LUDOX AS40 colloidal silica. IBH software was used for the decay analysis. Decays were fitted to get a symmetric distribution keeping χ^2 value at $0.99 \leq \chi^2 \leq 1.37$. Average fluorescence lifetime (τ_{aveg}) was calculated using the following equation⁴² where τ_i is the lifetime of i-th component with amplitude β_i , where n signifies number of components present.

$$\tau_{average} = \frac{\sum_{i=1}^n \beta_i \tau_i}{\sum_{i=1}^n \beta_i}$$

The desired temperature was controlled by using water circulation through jacketed cuvette holder from a refrigerated bath (Julabo, Germany).

Results and Discussion:

Synthesis of (*E*)-1-(galactose- β -(1 \rightarrow 4)- β -D-glucopyranosyl)-4-(1-pyrene)-but-3-en-2-one, (pyd-lact). To a solution of β -C-glycosidic ketone, **1** (1 mmol) in dry DCM were added pyrrolidine (30% mol) and 1-pyrenecarboxaldehyde, **2** (1.2 mmol).⁴³ After stirring at room temperature for 20h, the reaction mixture was evaporated under reduced pressure and extracted by EtOAc-water. The ethylacetate layer was dried over anhydrous Na₂SO₄ and concentrated to dryness. The product was further purified by flash column chromatography.



Scheme 1: Synthesis of (*E*)-1-(galactose- β -(1 \rightarrow 4)- β -D-glucopyranosyl)-4-(1-pyrene)-but-3-en-2-one, (pyd-lact).

Photo-physical studies of (*E*)-1-(galactose- β -(1 \rightarrow 4)- β -D-glucopyranosyl)-4-(1-pyrene)-but-3-en-2-one (pyd-lact) in homogeneous media. Absorption spectra of pyd-lact in different solvents are given in Figure 2a. Absorption spectra of pyd-lact are red shifted (\sim 380 nm) as compared to that of pyrene (\sim 340 nm) due to the double bond and keto conjugation. The extension of conjugation of pyrene chromophore through the α,β -unsaturated carbonyl group causes significant blurring² of the vibrational fine structure of the parent pyrene chromophore.^{24,44} In addition to this spectral broadening there could be the possibility of charge transfer interaction in polar solvents which give rise to the peak with a shoulder. Unlike pyrene-3-carboxaldehyde, absorption spectra of pyd-lact show minor perturbation towards solvent polarity. Here, pyd-lact exhibits a bathochromic shift of \sim 17 nm from methanol (361 nm) to water (378 nm). The longer wavelength onset of the absorbance spectrum in water signifies the presence of ground state charge transfer forms. Figure 2b shows emission spectra of pyd-lact in solvents of different polarity. In normalized spectra (inset of Figure 2b), emission of pyd-lact shows a red shift of \sim 96 nm from THF (dielectric constant 7.6) to water (dielectric constant 80.1). Similar positive solvatochromism is also found in pyrene-3-carboxaldehyde.² But, in pyd-lact fluorescence emission is much red shifted compared to pyrene-3-carboxaldehyde. This could be due to the extended π electron delocalization through the double bond to the carbonyl moiety. A small signature of structured band at shorter wavelength indicates local emission, in addition to the red shifted charge transfer emission.² The phenomenon of charge transfer has been observed in time dependent density function theory (TDDFT) calculation using Gaussian 09.⁴⁵ The bulky lactose moiety has been replaced with a small methyl group for reducing computational cost. The optimized ground state geometry in gas phase shows that pyrene is not planer with α,β -unsaturated carbonyl group (Figure 3a). The frontier molecular orbital

calculation using B3LYP/6-31G(d)⁴⁶ depicts that the HOMO of pyd-lact is more localized over the pyrene ring and the LUMO is more localized on the α,β -unsaturated carbonyl moiety (Figure 3b). This hints at the possibility of ICT (intramolecular charge transfer). In literature it is known that pyrene ring may act as either a donor or an acceptor depending on the substituent present. From the figure 3b it is evident that pyrene is donor and α,β -unsaturated carbonyl group behaves as an acceptor.⁴⁷ The highest separation of the local and ICT band (Figure 2b) is found in water due to its high polarity (dielectric constant 80.1). In case of derivatives (e.g. pyrene-3-carboxaldehyde, 1-acetylpyrene etc.), where pyrene is directly attached with carbonyl moieties proximity effect of $n-\pi^*$ and $\pi-\pi^*$ state was used for explaining the fluorescence and its solvatochromic shift.^{2,5}

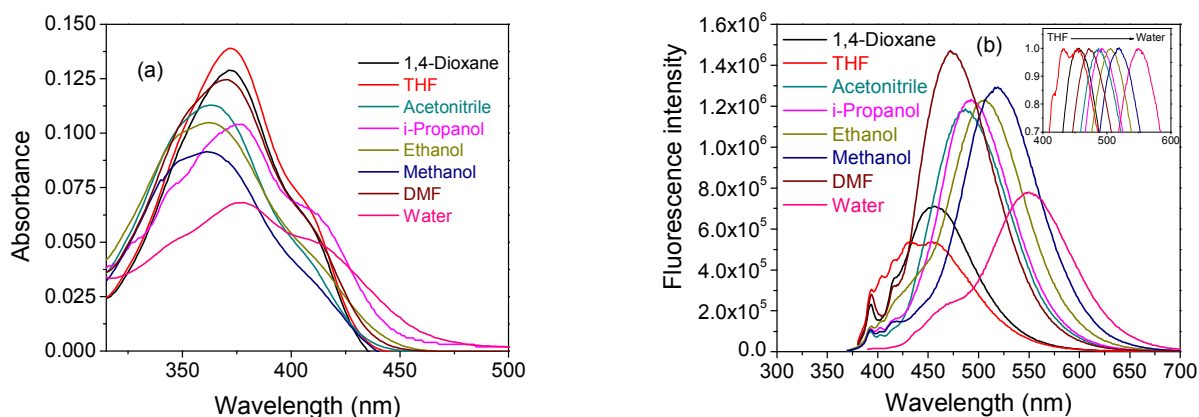


Figure 2: (a) Absorption spectra and (b) fluorescence spectra of pyd-lact, inset shows normalized emission spectra at 10 μ M in solvents of different polarity.

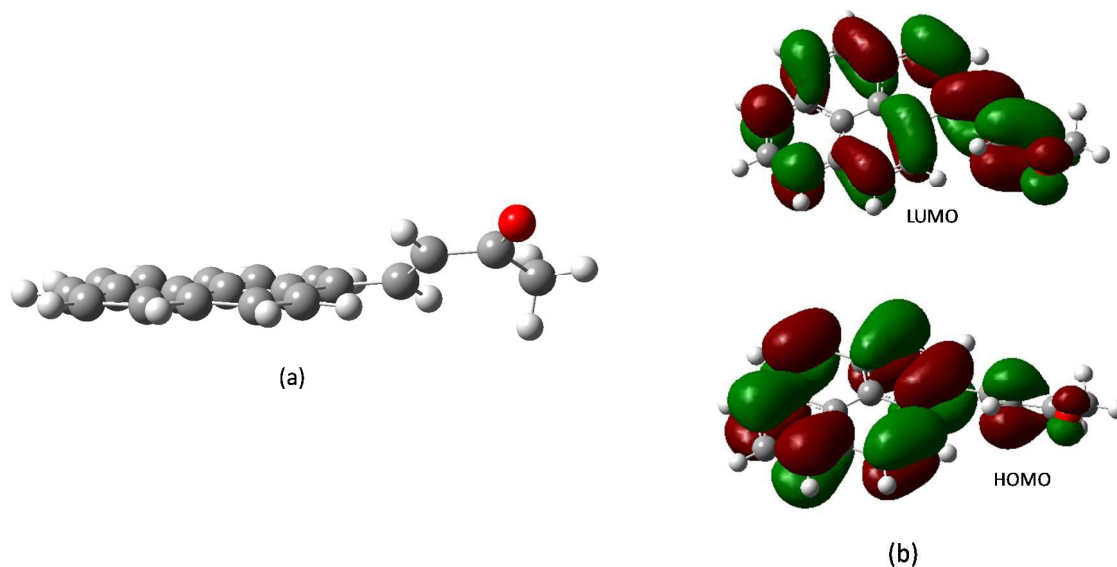


Figure 3: (a) Ground state optimized structure and (b) HOMO and LUMO of pyd-lact from B3LYP/6-31G(d), in gas phase.

Solvatochromic shift of the charge transfer emission band of pyd-lact has been fitted in several solvent parameter scales.^{42,48} Lippert-Mataga plot has been made (Figure 4a) according to the following equation,⁴²

$$\bar{\nu}_A - \bar{\nu}_F = \frac{2}{hc} \left(\frac{\epsilon - 1}{2\epsilon + 1} - \frac{n^2 - 1}{2n^2 + 1} \right) \frac{(\mu_E - \mu_G)^2}{a^3} + \text{constant}$$

here, $\bar{\nu}_A$ and $\bar{\nu}_F$ are the wavenumbers (cm^{-1}) of absorption and emission maxima, respectively, h is Planck's constant, c is the speed of light, ϵ is dielectric constant of the medium, n is refractive index of the solvent, a is radius of the cavity occupied by the fluorophore, μ_E and μ_G are the dipole moments of the fluorophore in excited state and ground state, respectively. In Lippert-

Mataga plot, Stokes' shift is plotted against the orientation polarisability (Δf), which defines as follows,

$$\Delta f = \frac{\varepsilon - 1}{2\varepsilon + 1} - \frac{n^2 - 1}{2n^2 + 1}$$

Linearity of the Lippert-Mataga plot indicates bulk polarity of solvents is responsible for the red shift of emission maxima rather than any kind of specific interaction. Non-linearity of 1,4-dioxane observed in this plot is due to its quadrupole moment.⁴⁹ Although 1,4-dioxane is a non-polar molecule, high quadrupole moment of its chair conformation and high polarity of its boat conformation increase solute-solvent interaction. As a result, it behaves as a pseudo-polar solvent.⁴⁹ In Figure 4b solvatochromic shift of pyd-lact emission maxima has been fitted with respect to the Kosower's Z value.⁴⁸ Unlike Lippert-Mataga plot, Kosower's plot is a single parameter approach which also shows linear plot. Similar correlation with solvent polarity has also been found in case of pyrene-3-carboxaldehyde.³ In the previously introduced molecule, pyd-glc, the essential fluorophore is the basic pyrene moiety and hence the intensity ratio of $I_{\text{I}}/I_{\text{III}}$ could be used as a photophysical parameter for polarity sensing.²⁴ For the present molecule pyd-lact, however, the extension of conjugation results in significantly different photophysical properties. Thus the emission spectrum is structure less and broad. The solvatochromic shift of the emission (Figure 4) indicates charge transfer character of the emission band which can be used to follow the micro-polarity of organized media. Photo-physical studies using binary solvents have also been done with 1,4-dioxane and water (Supporting Information, Figure S1). It shows a gradual shift of emission maxima towards red with the gradual increase in dielectric constant of the solvent mixture (normalized spectra, inset of Supporting Information, Figure S1).

This experiment further shows the effect of general solvation is responsible for the solvatochromic shift of the charge transfer band.

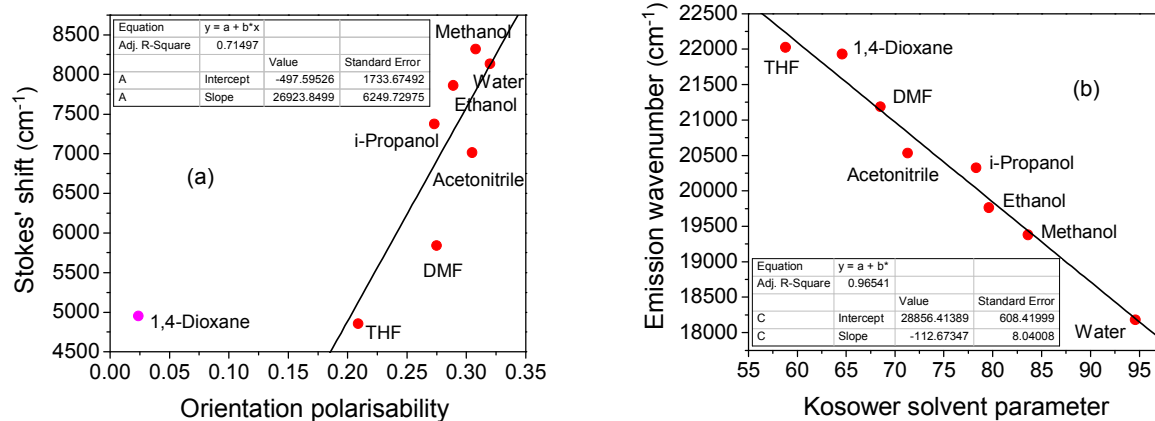


Figure 4: (a) Lippert-Mataga plot and (b) Kosower plot for pyd-lact.

Interaction study of pyd-lact with β -CD. β -cyclodextrin (CD) having a cavity diameter 6.2 Å and length 8.0 Å, is known to accommodate one pyrene molecule in its larger side.^{3,31,35} As pyd-lact has a pyrene moiety it is expected to respond in presence of β -CD. Figure 5a shows the change in emission spectra of pyd-lact with increasing concentration of β -CD. When the molecule is encapsulated in the cavity of β -CD it experience more hydrophobic environment as a result of this, longer wavelength ICT band shifts towards blue with intensity enhancement and merge with the shorter wavelength local emission band. Inset of Figure 5a shows the normalized spectra of the same which shows blue shift of emission maxima. A gradual hypsochromic shift of ~ 40 nm (Figure 5b) has been found due to pyrene's new location inside the β -CD nano-cavity. As in the presence of host molecule (β -CD), guest molecule (pyd-lact) goes into the hydrophobic cavity provided by the host leaving the aqueous solvation sphere. Dielectric constant (ϵ) of β -CD cavity is 48, which is much lower as compared to water ($\epsilon = 80$). As a result, pyd-lact experience a much lower polarity in presence of β -CD resulting in the blue shift of emission maxima.^{3,50}

From the value of emission maxima micro-polarity of β -CD cavity has been determined by using the linear plot of Kosower Z scale (Supporting Information Figure S2). At 16 mM β -CD concentration, Kosower Z value is found to be ~ 81.74 for pyd-lact which resembles with the methanolic medium. An increase of fluorescence intensity by two times (Figure 5b) has also been found with increasing β -CD concentration. Figure 5c shows the variation of steady state fluorescence anisotropy (r_{ss}) with increasing β -CD concentration. pyd-lact shows marked change in anisotropy value due to the allowed fluorescence transition of α,β -unsaturated carbonyl conjugated pyrene. But in contrast, anisotropy was an insensitive parameter for the previous molecule, pyd-glc due to the forbidden emission of basis pyrene unit. Increase in anisotropy signifies pyrene moiety of pyd-lact is in more rigid environment as compare to the aqueous medium. The most probable scheme for pyd-lact - β -CD complex has been shown in Figure 5d, where pyrene ring goes inside axially keeping its large disaccharide ring outside. Literature reports also support the inclusion of pyrene into β -CD cavity in this manner.³⁵ Reports show that, at moderate concentration, β -CD forms 1:1 complex with pyrene, which has been proven by lifetime data and CPK space filling model.³⁵ Having a length of 10.4 Å and width of 8.2 Å pyrene cannot enter into β -CD cavity fully like γ -CD, only part of it goes inside in the following manner.³⁵

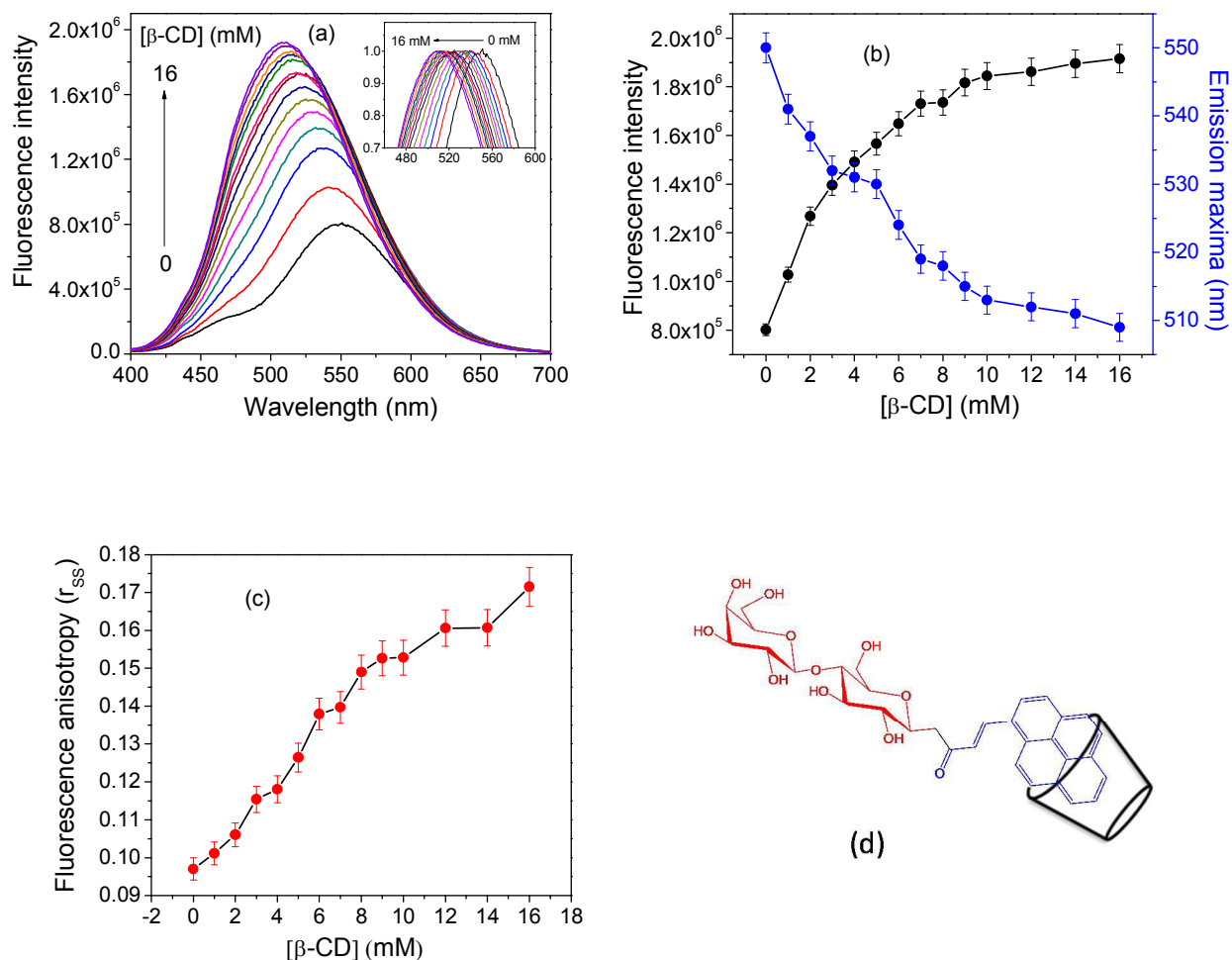


Figure 5: (a) Fluorescence spectra of pyd-lact (10 μM) with increasing concentration of $\beta\text{-CD}$, inset shows its normalized spectra, variation of (b) fluorescence intensity and emission maxima and (c) steady state fluorescence anisotropy (r_{ss}) of pyd-lact with increasing $\beta\text{-CD}$ concentration, at λ_{ex} 380 nm and (d) probable scheme for the penetration of pyd-lact inside $\beta\text{-CD}$ cavity.

Inclusion constant of the host-guest complex has been determined by the following non-linear scattering method.³²

$$\frac{1}{(I - I_0)} = \frac{1}{(rC)} + \frac{1}{(rCK_i [CD])}$$

where, I_0 and I are the intensities of the probe in absence and presence of $\beta\text{-CD}$, r is the constant, C is concentration of guest molecule, here pyd-lact (10 μM), K_i is the inclusion constant, $[CD]$ is

the concentration of β -CD. From this equation, it is clear that inclusion constant (K_i) can be determined from slope/intercept value of the straight line obtained by plotting $1/[CD]$ vs. $1/(I - I_0)$, as shown in Figure 6. From this plot the value of K_i is obtained to be $(240 \pm 10) M^{-1}$ at room temperature. This value for pyd-lact is comparable well with Rutin, a sugar containing flavone.³⁴ The perfect linearity ($R^2 = 0.9961$) shows exclusive presence of 1:1 inclusion complex. The inclusion constant value of pyd-lact is lower ($K_i = 240 M^{-1}$) as compared to the previously introduced probe, pyd-glc ($K_i = 550 M^{-1}$).²⁴ This is possibly due to the higher hydrophilicity of the lactose group as well as the bulkiness of disaccharide lactose molecule in pyd-lact as compared to the protected glucose in pyd-glu.

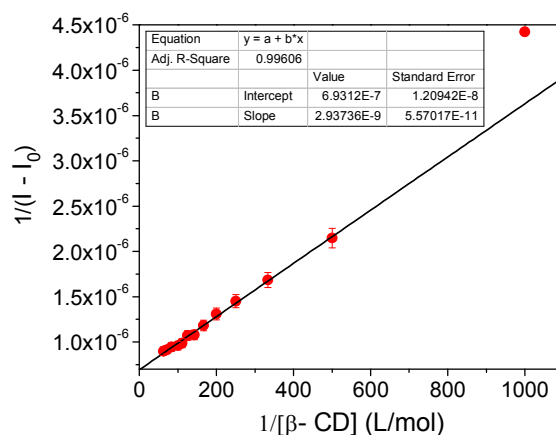


Figure 6: Determination of inclusion constant of pyd-lact in β -CD cavity at room temperature.

The indication of encapsulation of pyd-lact in β -CD cavity has also been obtained from the absorbance study (Supporting Information, Figure S3). It has been found that, on the addition of 16 mM β -CD into the aqueous solution of pyd-lact there is a ~ 40 nm blue shift (500 nm for water and 460 nm for 16 mM β -CD solution) in the onset of the absorbance spectrum. This

indicates the encapsulation of pyd-lact inside the β -CD cavity due to which the probe is experiencing much hydrophobic environment. As a result of this, the red shifted onset of the charge transfer absorbance in water is undergoing hypsochromic shift. Along with that, there is a clear isosbestic point at 427 nm which indicates the two state equilibrium of pyd-lact in water and in β -CD cavity at the ground state.

Figure 7 shows fluorescence lifetime decay profiles of pyd-lact with increasing β -CD concentration. Table S1 in Supporting Information summarizes the fluorescence lifetime values with increasing concentration of β -CD, at $\lambda_{\text{ex}} = 370$ nm. Residue distribution plots for the same have been given in Supporting Information, Figure S4. Bi-exponential decay of fluorescence lifetime is due to the presence of both local and ICT state which are very difficult to be assigned.² So for simplicity, average fluorescence lifetime has been calculated and used for further analysis. Moreover, the extension of conjugation lifts the S_0 - S_1 transition forbidden-ness of pyrene, thereby decreasing the fluorescence lifetime of pyd-lact.⁴⁷ The two fold increase in average fluorescence lifetime (τ_{aveg}) value (inset of Figure 7) is parallel with the increase in fluorescence intensity. The average fluorescence lifetime increases due to the new location of pyd-lact into the hydrophobic β -CD nano-cavity that reduces non-radiative decay.

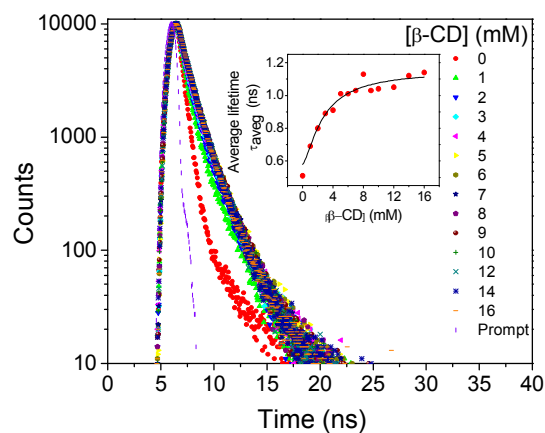
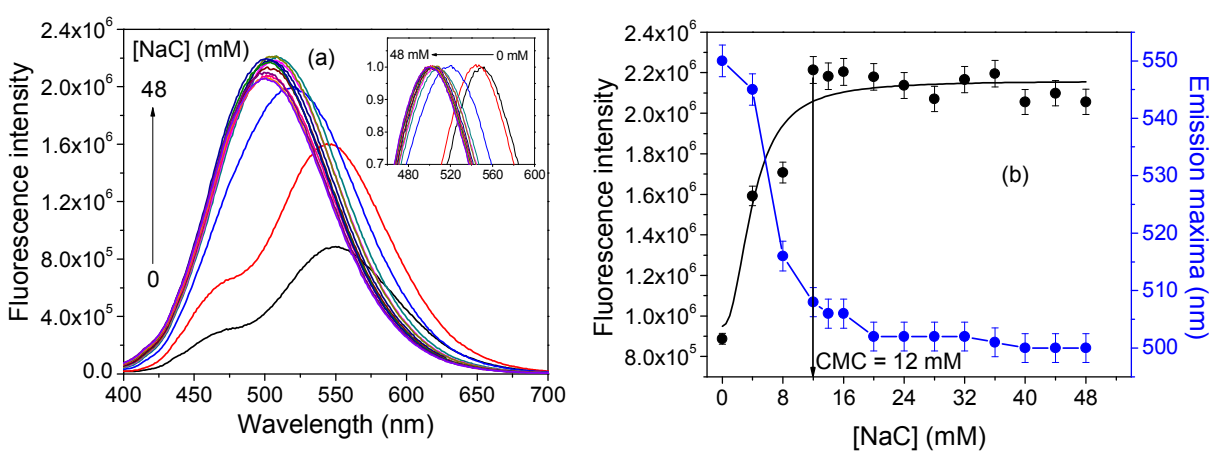


Figure 7: Fluorescence lifetime decay profiles of pyd-lact with increasing concentration of β -CD, inset shows variation of average fluorescence lifetime with increasing β -CD concentration, $\lambda_{\text{ex}} = 370$ nm.

Interaction of pyd-lact with bile salts (NaC, NaDC). With increasing bile salt concentration monomeric units of bile salt start aggregating forming primary aggregates followed by the formation of secondary aggregates at higher concentration.³⁸ Sodium cholate (NaC) and sodium deoxycholate (NaDC) are the examples of bile salts having critical micellar concentration (CMC) 12-16 and 4-6 mM, respectively.³⁸ Here, pyd-lact has been used as a sensor of micro-polarity induced by the aggregation of bile salts. Figure 8a and c show the change in fluorescence spectra with increasing concentration of NaC and NaDC, respectively. The longer wavelength ICT emission of pyd-lact shifts towards the shorter wavelength LE emission with intensity enhancement in presence of hydrophobic bile salt environment and finally merges to a single peak. Inset of Figure 8a and c are the respective normalized spectra. With increasing bile salt concentration blue shift of the emission maxima has been found due to the progressive micellization of bile salt media as shown in Figure 8b and d. Enhancement of fluorescence intensity follows the critical micellar concentration of the respective bile salts (Figure 8b and d). Figure 8e shows the change of steady state fluorescence anisotropy (r_{SS}) as a function of NaC and NaDC concentration. Anisotropy arises due to the extended π -conjugation and it shows onset

at the critical micellar concentration. This has not been found in case of the previously introduced molecule, pyd-glc with basis pyrene moiety. From Figure S2 in Supporting Information, polarity of the post micellar bile salt media has been calculated using Kosower Z plot. Kosower Z value has been found to be ~ 78.56 and 76.80 in NaC and NaDC media, respectively. It shows the location of pyd-lact in NaC and NaDC media is like EtOH and *i*-PrOH medium, respectively. Due to the hydrophilic character of pyd-lact it resides mostly inside the more polar cavity provided by the secondary aggregates of bile salts.⁵¹ The lower Z value in di-hydroxy NaDC media than tri-hydroxy NaC media gives an indication towards medium micro-polarity by pyd-lact.



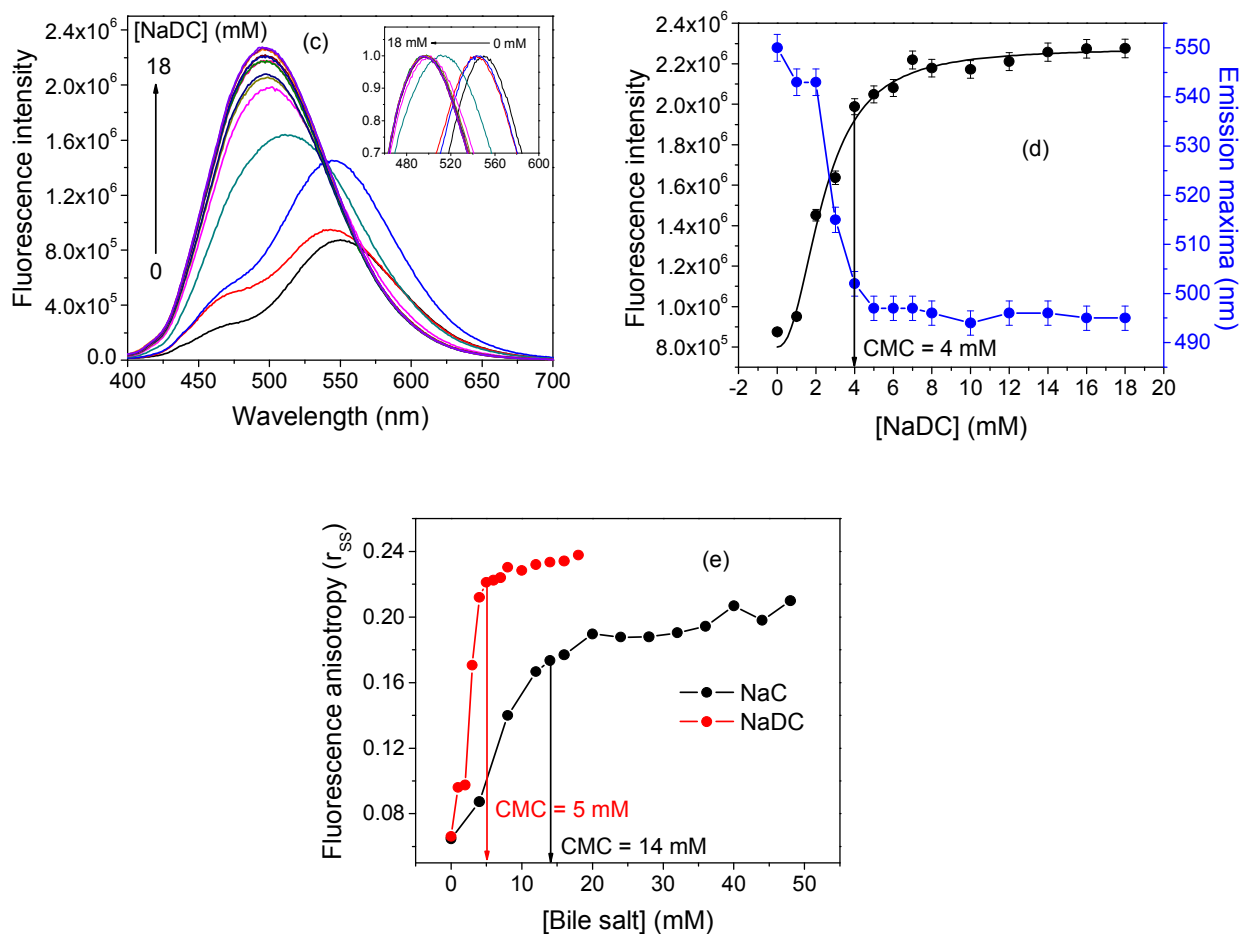


Figure 8: (a) Fluorescence spectra of pyd-lact (10 μM) with increasing concentration of NaC, inset shows normalized spectra, (b) variation of fluorescence intensity and emission maxima with NaC concentration, (c) Fluorescence spectra of pyd-lact (10 μM) with increasing concentration of NaDC, inset shows normalized spectra, (d) variation of fluorescence intensity and emission maxima with NaDC concentration, (e) variation of steady state fluorescence anisotropy (r_{SS}) of pyd-lact with increasing bile salt concentration, at λ_{ex} 380 nm.

Figure 9a and b show the fluorescence lifetime decay profiles of pyd-lact with micellization of NaC and NaDC, respectively. Table S2 and S3 in Supporting Information summarize the fluorescence lifetime data of pyd-lact with increasing NaC and NaDC concentration, respectively. Residue distribution plots for the same have been given in Supporting Information, Figure S5 and Figure S6. Similar bi-exponential decay of fluorescence lifetime has also been

obtained in bile salt media which has been averaged out for further analysis. Onsets of average fluorescence lifetime (τ_{aveg}) value occur at the respective CMCs (inset of Figure 9a, b)

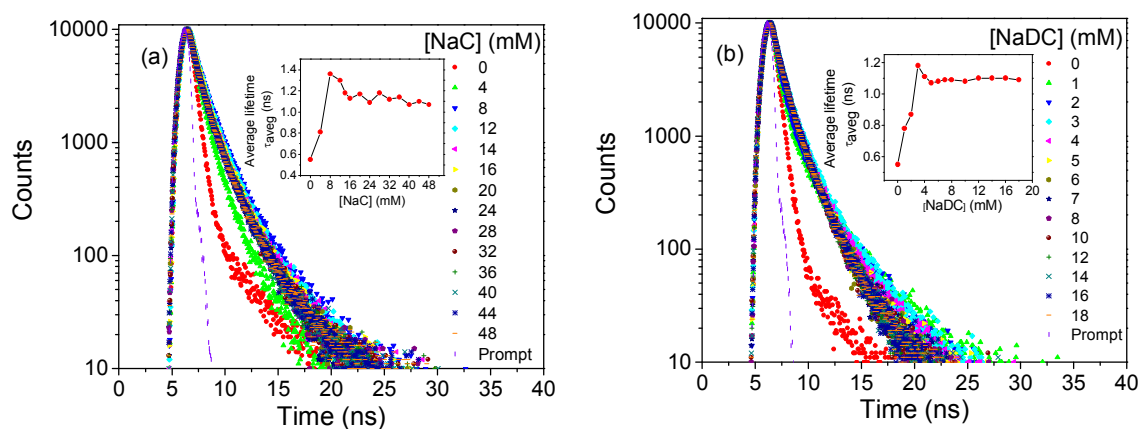
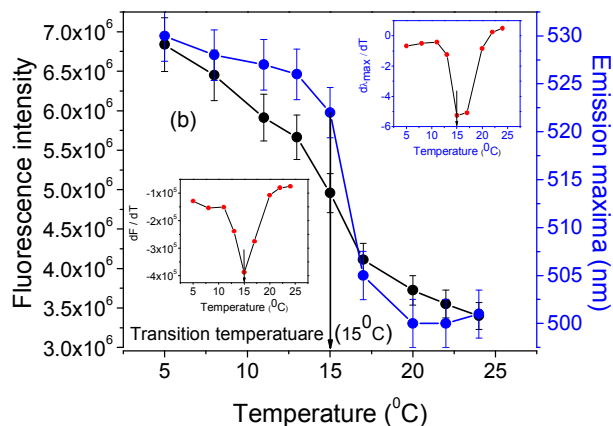
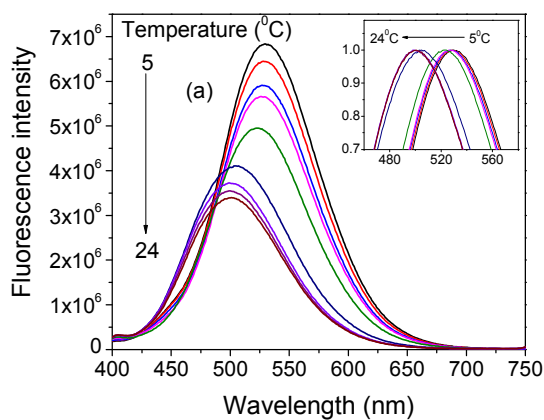


Figure 9: Fluorescence lifetime decay profiles of pyd-lact with increasing concentration of (a) NaC and (b) NaDC, at $\lambda_{\text{ex}} = 370$ nm.

Interaction of pyd-lact with 10% pluronic P123 as a function of temperature. The thermotropic sol-gel transition of highly industrially used block polymer pluronic P123 has been investigated using pyd-lact. This kind of polymers form micelle and gel both as a function of concentration and temperature.⁴¹ Although CMC value differs from batch to batch, this used concentration (10%) is far above the CMC of pluronic P123 at that temperature.^{41,52,53} Figure 10a shows the change in fluorescence spectra of pyd-lact in 10% P123 with temperature, inset shows its normalized form. A ~ 20 nm hypsochromic shift of emission maxima from water ($\lambda_{\text{em}} = 550$ nm) to the polymeric sol media ($\lambda_{\text{em}} = 530$ nm) has been found. Figure 10b shows the variation of fluorescence intensity and emission maxima of pyd-lact with sol-gel transition in P123 media. There is a sigmoidal decrease in the intensity and emission maxima as a function of temperature. In the respective derivative plots it show minima at 15°C which is the sol-gel transition temperature of 10% P123. The progressive dehydration of the micelle during sol-gel transition

increases hydrophobicity of the medium as a result, blue shift of emission maxima takes place.⁵⁴ Kosower Z value in sol state is 88.65 which indicates water-MeOH like environment, whereas, in gel state it senses non-polar EtOH like environment with Z value 78.95 (Supporting Information, Figure S2). Figure 10c shows the comparison of emission intensities of pyd-lact in pluronic P123 and water. In polymeric media there is almost 10 times increase in fluorescence intensity as compare to water. The intensity decrease of pyd-lact in pluronic P123 media shows a specific pattern unlike in water. Steady state fluorescence anisotropy (r_{SS}) also indicates sol-gel phase change (Figure 10d). As the polymeric system alters itself from hydrated sol state to dehydrated gel state there is a marked increase in fluorescence anisotropy. In the derivative plot (insets of Figure 10d) it shows maxima at the sol-gel transition temperature (15°C).



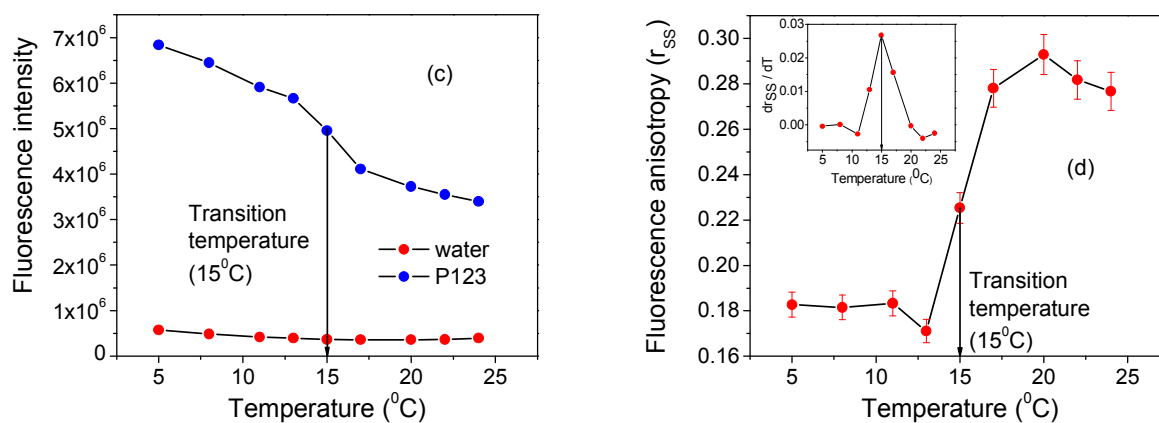


Figure 10: (a) Fluorescence spectra of pyd-lact (10 μ M) in 10% pluronic P123 with increasing temperature, inset shows normalized spectra, (b) variation of fluorescence intensity and emission maxima of pyd-lact in 10% pluronic P123 with increasing temperature, inset show derivative plots, (c) fluorescence intensity change of pyd-lact in water and pluronic P123 media with increasing temperature and (d) variation of steady state fluorescence anisotropy (r_{SS}) of pyd-lact in 10% pluronic P123 with increasing temperature, inset shows derivative plot, at λ_{ex} 380 nm.

Fluorescence lifetime decay profiles of pyd-lact in 10% pluronic P123 with temperature has been given in Figure 11a. Table S4 in Supporting information enlists the fluorescence lifetime data of pyd-lact in both water and pluronic P123 media at different temperatures. Residue distribution plots for the same have been given in Supporting Information, Figure S7. Average fluorescence lifetime of the bi-exponential decay has been used for analysis to avoid complication. Figure 11b compares the average fluorescence lifetime (τ_{avg}) values of pyd-lact in water and pluronic P123 media. This shows average fluorescence lifetime of pyd-lact in pluronic P123 is higher than the aqueous solution which supports the steady state data (Figure 10c). In pluronic P123, average fluorescence lifetime decreases with a particular pattern showing minima at the sol-gel transition temperature in its derivative plot (inset of Figure 11b).

Significant change in the above mentioned fluorescent parameters at sol-gel transition temperature (15°C) suggests the probable location of the probe inside the micelle.⁵⁵ Due to the attached lactose moiety with seven hydroxyl groups pyd-lact is a fairly hydrophilic molecule with an affinity for the interfacial region. As a result, it can be assumed that lactose moiety of pyd-lact remains in the corona region with the pyrene ring at core-corona interfacial region. Very high value of steady state fluorescence anisotropy (r_{ss}) in the gel phase supports this model.

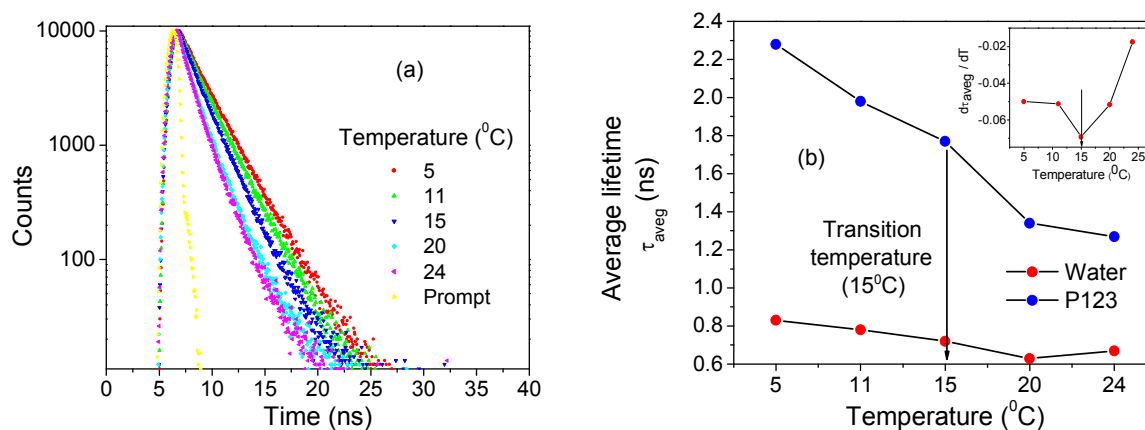


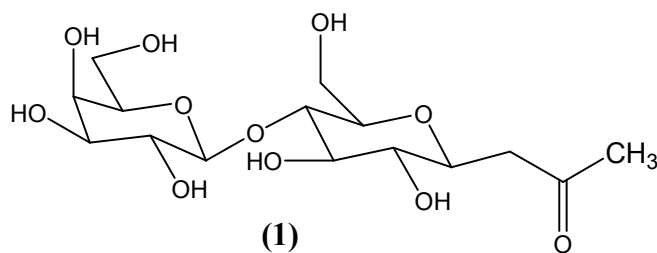
Figure 11: (a) Fluorescence lifetime decay profiles of pyd-lact in 10% pluronic P123 with increasing temperature and (b) average fluorescence lifetime of pyd-lact in both water and 10% pluronic P123 media, inset shows derivative plot of average fluorescence lifetime value in 10% pluronic P123 with temperature, at $\lambda_{\text{ex}} = 370 \text{ nm}$.

Conclusion:

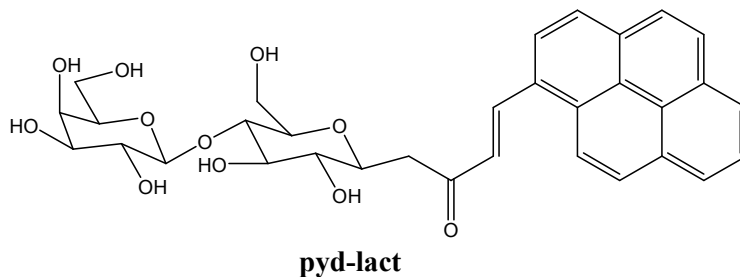
A detailed photo-physical study on the newly synthesized fluorescent molecular probe, (*E*)-1-(galactose- β -(1 \rightarrow 4)- β -D-glucopyranosyl)-4-(1-pyrene)-but-3-en-2-one, (pyd-lact) has been carried out in both homogeneous and micro-heterogeneous media. Electron withdrawing extended π -conjugation removes the emission forbidden-ness of pyrene which arises broad

charge transfer emission band for pyd-lact. As a result of this conjugation induced allowedness of the S_1-S_0 transition, anisotropy value comes as a key parameter to monitor the micro-heterogeneity, unlike pyd-glc with basis pyrene unit. Characteristics long fluorescence lifetime of pyrene decreases substantially due to this conjugation. Polarity dependent solvatochromic shift of the intramolecular charge transfer emission band of pyd-lact is like pyrene-3-carboxaldehyde and provides a useful parameter to determine medium polarity. This probe has been employed into sugar based β -CD media where it forms 1:1 complex with an inclusion constant value $(240 \pm 10) M^{-1}$ at room temperature. This value is fairly low as compared to the less bulky probe molecule, pyd-glc, which shows that the size of sugar molecule plays an important role in inclusion. Additionally, pyd-lact has been employed into the non-sugar based micro-heterogeneous bile salt and polymeric P123 media. pyd-lact has been found to follow the progressive micellar aggregation of natural surfactant, bile salts. Thermo-reversible sol-gel transition of tri-blocked pluronic P123 has also been monitored by this probe. Finally this work shows that, being a hydrophilic probe pyd-lact appears as a sensitive probe towards sensing the interfacial region of micro-heterogeneous media, whereas, common pyrene derivatives act as hydrophobic probes.

Experimental section:



Synthesis of 1-(galactose- β (1 \rightarrow 4)- β -D-glucofuranosyl)-propan-2-one (1**):** To a solution of D-lactose (3.82 g, 10 mmol) in 8:2 water-THF (10 ml) were added NaHCO₃ (3.36 g, 40 mmol) and 2,4-pentadienone (2.1 ml, 20 mmol). After stirring at 90 °C for about 24 h, followed by concentration to dryness under reduced pressure and fractionation by column chromatography with 3:7 (CHCl₃-MeOH) resulted in product, **1** as colorless crystals. M.p.: 152-155 °C; Yield : 67 %; ¹H NMR (CDCl₃): δ 4.31 (d, J =7.8 Hz, 1H, Sac-H), 3.46-3.79 (m, 10H, Sac-H), 3.41 (t, J = 8.7 Hz, 2H, Sac-H), 3.14 (t, J = 8.6 Hz, 1H, Sac-H), 2.89 (d, J = 16.8 Hz, 1H, Sac-H), 2.55-2.63 (dd, J = 16.7 Hz, J = 9.0 Hz, 1H, Sac-H), 2.14 (s, 3H, -COCH₃); ¹³C NMR (CDCl₃): δ 213.1 (Sac-C), 102.9 (Sac-C), 78.4 (Sac-C), 78.3 (Sac-C), 75.8 (Sac-C), 75.3 (Sac-C), 75.1 (Sac-C), 72.8 (Sac-C), 72.5 (Sac-C), 70.9 (Sac-C), 68.5 (Sac-C), 61.0 (Sac-C), 60.1 (Sac-C), 45.6 (Sac-C), 29.8 (-CH₃).



Synthesis of (E)-1-(galactose- β (1 \rightarrow 4)- β -D-glucofuranosyl)-4-(1-pyrene)-but-3-en-2-one, (pyd-lact): Compound, **pyd-lact** was obtained by the reaction of β -C-glycosidic ketone (**1**), (1 mmol, 0.382 g) and 1-pyrenecarboxaldehyde, (1.2 mmol, 0.276 g) as a yellow solid. M.p :227-229 °C. Yield: 80 %. ¹H NMR (300 MHz, TMS, ppm): δ 8.62-8.71 (m, 2H, Ar-H), 8.52 (d, J = 8.1 Hz, 1H, Ar-H), 8.19-8.37 (m, 6H, Ar-H), 8.11 (t, J = 7.8 Hz, 1H, Ar-H), 7.21 (d, J = 15.6 Hz, 1H, Alk-H), 5.46 (s, 1H, Sac-H), 4.88 (s, 3H, Sac-H), 4.59 (s, 2H, Sac-H), 4.25 (d, J = 6.0 Hz,

2H, Sac-H), 3.02-3.81 (m, 15H, Sac-H); ^{13}C NMR (75 MHz, TMS, ppm): δ 198.1, 138.2, 132.2, 130.8, 130.2, 129.4, 129.2, 128.6, 128.2, 127.3, 126.6, 126.1, 125.9, 125.3, 124.5, 124.0, 123.7, 122.6, 103.8, 80.9, 78.7, 76.2, 75.8, 75.5, 73.3, 73.2, 7.06, 68.1, 60.6, 60.3, 43.4. Elemental analysis Anal. Calc. for $\text{C}_{32}\text{H}_{34}\text{O}_{11}$: C, 64.64; H, 5.76 %. Found: C, 64.97; H, 5.60.

Associated Content:

Supporting Information. Fluorescence spectra of pyd-lact in water with increasing % of 1,4-dioxane, Determination of the medium polarity from λ_{em} value using Kosower Z scale for β -CD, bile salts and pluronics media, Absorbance spectra of pyd-lact in water and β -CD, Fluorescence lifetime data of pyd-lact with increasing β -CD concentration, Residue distribution plot of pyd-lact in β -CD. Fluorescence lifetime data of pyd-lact with increasing NaC concentration. Fluorescence lifetime data of pyd-lact with increasing NaDC concentration. Residue distribution plot of pyd-lact in NaC. Residue distribution plot of pyd-lact in NaDC. Fluorescence lifetime data of pyd-lact in water and 10% pluronic P123 with increasing temperature. Residue distribution plot of pyd-lact in water and 10% pluronic P123 with temperature. ^1H NMR spectrum of pyd-lact. ^1H NMR expansion spectrum of pyd-lact. ^{13}C NMR spectrum of pyd-lact.

Acknowledgment:

A. K. M. thanks DST, Government of India for financial assistance in the form of major project. T. M. acknowledge SERC-DST, New Delhi for financial support. T. M. thank DST, New Delhi for use of NMR facility under DST-FIST programme to the Department of Organic Chemistry, University of Madras, Guindy Campus, Chennai, India. I. S. and A. H. thank CSIR, New Delhi,

India for their research fellowships. Finally, we want to acknowledge Mr. Avik Kumar Pati, Senior Research Fellow in IIT Madras for Gaussian calculations.

Reference:

- 1 S. M. Meyerhoffer and L. B. McGown, *Anal. Chem.*, 1991, **63**, 2082–2086.
- 2 Y. Niko, Y. Hiroshige, S. Kawauchi and G. Konishi, *Tetrahedron*, 2012, **68**, 6177–6185.
- 3 K. W. Street and W. E. Acree, *Appl. Spectrosc.*, 1988, **42**, 1315–1318.
- 4 P. Banerjee, S. Chatterjee, S. Pramanik and S. C. Bhattacharya, *Colloids Surfaces A Physicochem. Eng. Asp.*, 2007, **302**, 44–50.
- 5 S. Pankasem and J. K. Thomas, *J. Phys. Chem.*, 1991, **95**, 7385–7393.
- 6 M. Adeli, A. K. Fard, F. Abedi, B. K. Chegeni and F. Bani, *Nanomedicine Nanotechnology Biol. Med.*, 2013, **9**, 1203–1213.
- 7 E. Grueso and R. P. Gotor, *Chem. Phys.*, 2010, **373**, 186–192.
- 8 K. Kalyanasundaram and J. K. Thomas, *J. Phys. Chem.*, 1977, **81**, 2176–2180.
- 9 B. Valeur, *Molecular Fluorescence: Principles and Applications*, Wiley-VCH Verlag GmbH, 2001.
- 10 S. Nagarajan and T. M. Das, *New J. Chem.*, 2009, **33**, 2391–2396.
- 11 P. Somerharju, *Chem. Phys. Lipids*, 2002, **116**, 57–74.
- 12 V. W. Cornish, D. R. Benson, C. A. Altenbach, K. Hideg, W. L. Hubbell and P. G. Schultz, *Proc. Natl. Acad. Sci. U. S. A.*, 1994, **91**, 2910–2914.
- 13 M. G. Mendoza, M. L. Marin and M. A. Miranda, *J. Phys. Chem. Lett.*, 2011, **2**, 782–785.

- 14 H. Raghuraman, S. Shrivastava and A. Chattopadhyay, *Biochim. Biophys. Acta*, 2007, **1768**, 1258–1267.
- 15 H. S. P. Rao, A. Desai, I. Sarkar, M. Mohapatra and A. K. Mishra, *Phys. Chem. Chem. Phys.*, 2014, **16**, 1247–1256.
- 16 C. Huo, J. C. Chambron and M. Meyer, *New J. Chem.*, 2008, **32**, 1536-1542.
- 17 U. Schramm, A. Dietrich, S. Schneider, H. P. Buscher, W. Gerok and G. Kurz, *J. Lipid Res.*, 1991, **32**, 1769–1779.
- 18 B. E. Cohen, T. B. McAnaney, E. S. Park, Y. N. Jan, S. G. Boxer and L. Y. Jan, *Science*, 2002, **296**, 1700–1703.
- 19 K. Matsumoto, Y. Shinohara, S. S. Bag, Y. Takeuchi, T. Morii, Y. Saito and I. Saito, *Bioorganic Med. Chem. Lett.*, 2009, **19**, 6392–6395.
- 20 J. J. Li, R. Geyer and W. Tan, *Nucleic Acids Res.*, 2000, **28**, i-vi.
- 21 M. G. O’Shea, M. S. Samuel, C. M. Konik and M. K. Morell, *Carbohydrate Research*, 1998, **307**, 1-12.
- 22 M. C. Breadmore, E. Hilder and A. Kazarian, *Fluorophores and Chromophores for the Separation of Carbohydrates by Capillary Electrophoresis*, Capillary Electrophoresis of Carbohydrates, 2011, pp 23-51.
- 23 M. Becuwe, D. Landy, F. Delattre, F. Cazier and S. Fourmentin, *Sensors*, 2008, **8**, 3689-3705.
- 24 I. Sarkar, H. Malini, T. M. Das and A. K. Mishra, *RSC Adv.*, 2015, **5**, 64604–64613.
- 25 A. Jana, S. Atta, S. K. Sarkar and N. D. P. Singh, *Tetrahedron*, 2010, **66**, 9798-9807.
- 26 F. Hauke, A. Hirsch, S. Atalick and D. Guldi, *Eur. J. Org. Chem.*, 2005, 1741–1751.
- 27 B. H. Milosavljevic and J. K. Thomas, *J. Phys. Chem.*, 1988, **92**, 2997-3001.

- 28 F. K. Su, G. F. Liao and J. L. Hong, *J. Polym. Sci. Part B Polym. Phys.*, 2007, **45**, 920–929.
- 29 E. Miller and D. J. Styczynska, *Spectrochimica Acta Part A*, 2009, **72**, 312–321.
- 30 E. Biavardi, G. Battistini, M. Montalti, R. M. Yebetchou, L. Prodi and E. Dalcanale, *Chem. Commun.*, 2008, 1638–1640.
- 31 A. Y. Will, A. M. Pena, T. T. Ndou and I. M. Warner, *Appl. Spectrosc.*, 1993, **47**, 277–282.
- 32 H. X. Zhang, X. Huang, P. Mei, K. H. Li and C. N. Yan, *J. Fluoresc.*, 2006, **16**, 287–294.
- 33 G. C. Catena and F. V Bright, *Anal. Chem.*, 1989, **61**, 905–909.
- 34 M. R. Guzzo, M. Uemi, P. M. Donate, S. Nikolaou, A. E. H. Machado and L. T. Okano, *J. Phys. Chem. A*, 2006, **110**, 10545–10551.
- 35 A. M. Pena, T. Ndou, J. B. Zung and I. M. Warner, *J. Phys. Chem.*, 1991, **95**, 3330–3334.
- 36 G. Sugihara, K. Yamakawa, Y. Murata and M. Tanaka, *J. Phys. Chem.*, 1982, **86**, 2784–2788.
- 37 J. Tamminen and E. Kolehmainen, *Molecules*, 2001, **6**, 21–46.
- 38 S. Selvam and A. K. Mishra, *Photochem. Photobiol. Sci.*, 2011, **10**, 66–75.
- 39 E. V. Batrakova and A. V. Kabanov, *J. Control. Release*, 2008, **130(2)**, 98–106.
- 40 A. V. Kabanov, E. V. Batrakova and V. Y. Alakhov, *J. Control. Release*, 2002, **82**, 189–212.
- 41 M. E. Mohanty, V. J. Rao and A. K. Mishra, *Spectrochim. Acta - Part A Mol. Biomol. Spectrosc.*, 2014, **121**, 330–338.

- 42 J. R. Lakowicz, *Principles of Fluorescence Spectroscopy*, Kluwer Academic, Plenum Publishers, New York, 1999.
- 43 S. Nagarajan, T. M. Das, P. Arjun and N. Raaman, *J. Mater. Chem.*, **2009**, *19*, 4587-4596.
- 44 F. M. Winnik, *Chem. Rev.*, 1993, **93**, 587-614.
- 45 M. J. Frisch, G. W. Trucks, H. B. Schlegel, G. E. Scuseria, M. A. Robb, J. R. Cheeseman, G. Scalmani, V. Barone, B. Mennucci, G. A. Petersson et al., *Gaussian 09*, Revision C.01; Gaussian, Inc.: Wallingford, CT, 2010.
- 46 A. D. Becke, *J. Chem. Phys.*, 1993, **98**, 5648–5652.
- 47 A. K. Pati, S. J. Gharpure and A. K. Mishra, *Faraday Discuss.*, 2014, **177**, 1–23.
- 48 *Handbook of Photochemistry*, Taylor & Francis Group, LLC, 2006.
- 49 E. M. S. Castanheira and J. M. G. Martinho, *Chem. Phys. Lett.*, 1991, **185**, 319–323.
- 50 A. M. Pena, T. T. Ndou, J. B. Zung, K. L. Greene, D. H. Live and I. M. Warner, *J. Am. Chem. Soc.*, 1991, **113**, 1572–1577.
- 51 M. C. Cuquerella, J. Rohacova, M. L. Marin and M. A. Miranda, *Chem. Commun.*, 2010, **46**, 4965–4967.
- 52 P. Alexandridis, J. F. Holzwarth and T. A. Hatton, *Macromolecules*, 1994, **27**, 2414–2425.
- 53 G. Wanka, H. Hoffmann and W. Ulbricht, *Macromolecules*, 1994, **27**, 4145-4159.
- 54 J. J. Escobar-Chavez, M. Lopez-Cervantes, A. Naik, Y. N. Kalia, D. Quintanar-Guerrero and A. Ganem-Quintanar, *J. Pharm. Pharm. Sci.*, 2006, **9**, 339-358.
- 55 S. George, M. Kumbhakar, P. K. Singh, R. Ganguly, S. Nath and H. Pal, *J. Phys. Chem. B*, 2009, **113**, 5117–5127.

Introduction of a α,β -unsaturated carbonyl conjugated pyrene-lactose hybrid as a fluorescent molecular probe for micro-scale anisotropic media

Ivy Sarkar^a, Arasappan Hemamalini^b, Thangamuthu Mohan Das^{*b,c}, Ashok Kumar Mishra^{*a}

^a Department of Chemistry, Indian Institute of Technology Madras, Chennai – 600 036, India

^b Department of Organic Chemistry, University of Madras, Guindy Campus, Chennai - 600 025, India

^c Department of Chemistry, School of Basic and Applied Sciences, Central University of Tamil Nadu, Thiruvarur – 610 101, India

Graphical Abstract:

